

Hot topic E: Permeability: From in vitro best practices to in vivo relevance

“Measurement of the membrane permeability to drug candidates has helped reduce the pharmacokinetically related drug attrition rates from 40% to 10%”

1. Chipot C in: Predictions from First-Principles of Membrane Permeability to Small Molecules: How Useful Are They in Practice? J Chem Inf Model. 2023 Aug 14;63(15):4533-4544.
2. Kolal, Landis J. Can the pharmaceutical industry reduce attrition rates? Nat Rev Drug Discov. 2004;3:711–716.
3. Lipinski CA, Lombardo F, Dominy BW, Feeney PJ. Experimental and computational approaches to estimate solubility and permeability in drug discovery and development settings, 2001. Adv Drug Deliv Rev. 2001;46(1-3):3–26.
4. Volpe DA. Application of methods suitability for drug permeability classification. AAPS J. 2010;12(4):670–678.

Hans Lennernäs, Ph.D., Professor

**Translational Drug Discovery and Development,
Department of Pharmaceutical Bioscience,
Uppsala University,
Sweden**



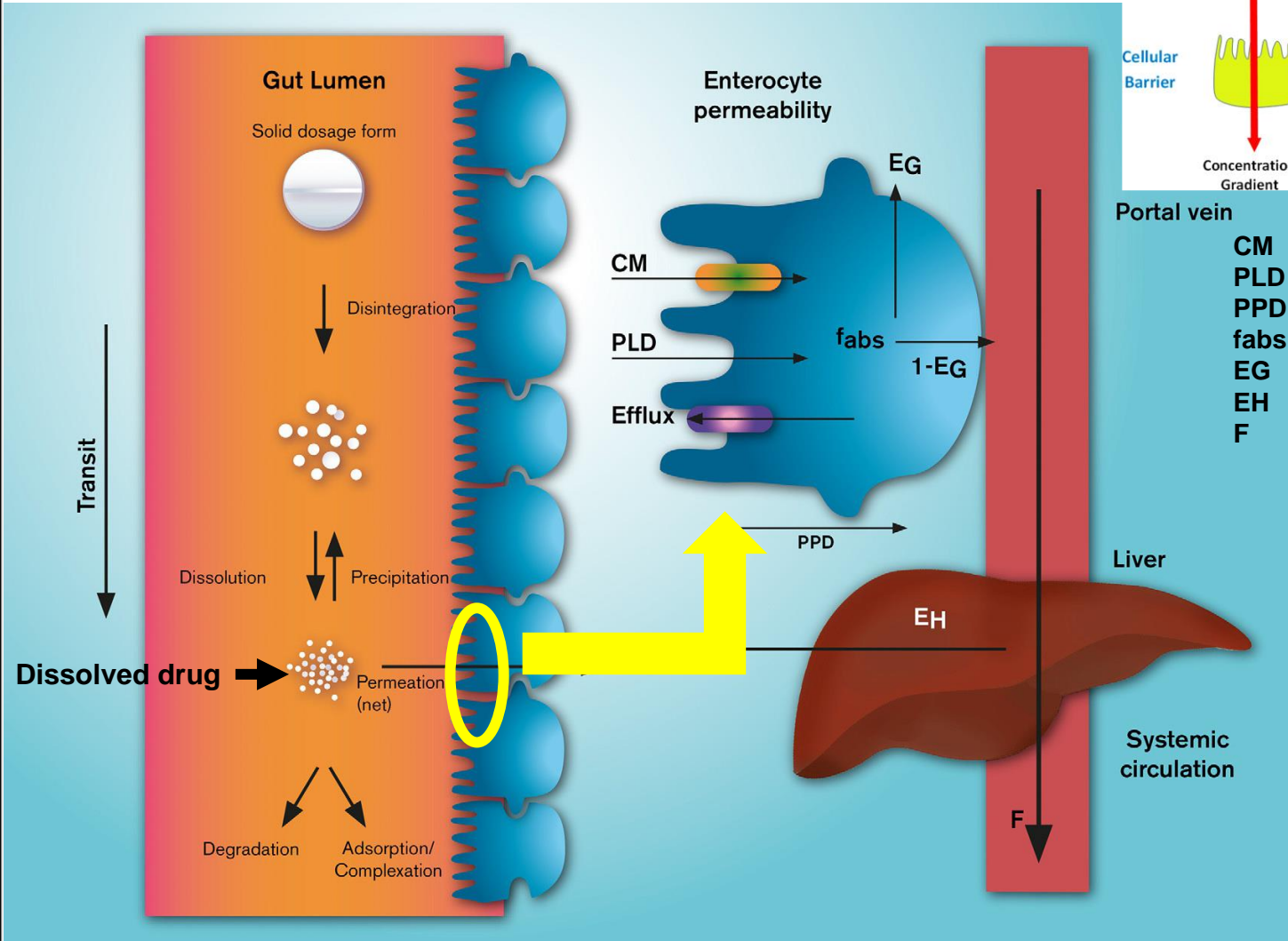
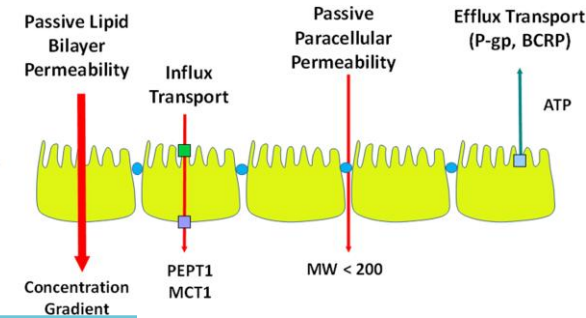


Outline of Today's lecture

- Human small and large intestinal permeability is the starting point –provides *in vivo* relevance for existing non-clinical and *in vitro* models as well as future more intestinal *in vitro* models.
- Experimental *in vitro* and non-clinical methods and comparisons for regional permeability
- Role of intestinal efflux *in vivo* and model predictions
- Future *In vitro* models with improved accuracy and precision?

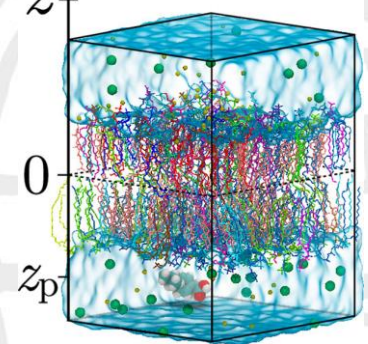
1. Doluisio JT, Billups NF, Dittert LW, Sugita ET, Swintosky JV. Drug absorption. I. An in situ rat gut technique yielding realistic absorption rates. J Pharm Sci. 1969;58(10):1196–200.
2. Doluisio JT, Tan GH, Billups NF, Diamond L. Drug absorption. II. Effect of fasting on intestinal drug absorption. J Pharm Sci. 1969;58(10):1200–2.
3. Ochsenfahrt H, Winne D. Der Einfluss des Wassernettoflusses auf die Resorption von Arzneimitteln [Influence of net flux of water on that absorption of drugs]. Naunyn Schmiedebergs Arch Pharmakol. 1970;266(4):414-5. German. PMID: 4253840.
4. Fogh, J., J.M. Fogh, and T.J.J.o.t.N.C.I. Orfeo, One hundred and twenty-seven cultured human tumor cell lines producing tumors in nude mice. Journal of the National Cancer Institute. 1977.
5. Hidalgo, I., T. Raub, and R. Borchardt, Characterization of the human colon carcinoma cell line (Caco-2) as a model system for intestinal epithelial permeability. Gastroenterology. 1989. 96(2): p. 736-749
6. Amidon GL, Lennernäs H, Shah VP, Crison JR. A theoretical basis for a biopharmaceutic drug classification: the correlation of in vitro drug product dissolution and in vivo bioavailability. Pharm Res. 1995 Mar;12(3):413-20. doi: 10.1023/a:1016212804288. PMID: 7617530.

In vivo relevance of *in vitro* permeability models – site of measurements



CM carrier mediated
PLD passive lipoidal diffusion
PPD passive paracellular diffusion
f_{abs} fraction absorbed
EG gut-wall extraction
EH hepatic extraction
F bioavailability

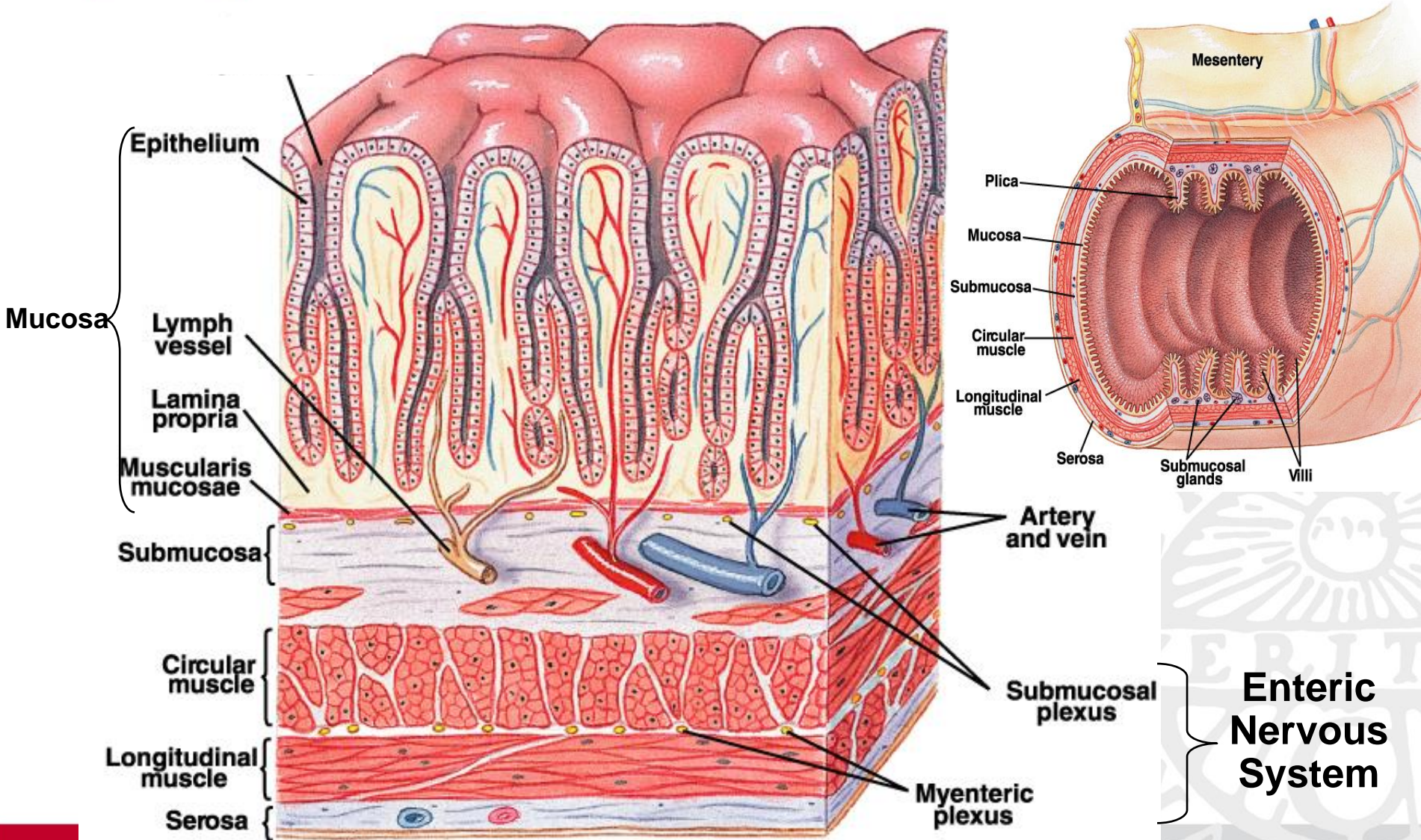
Lipidol Diffusion = Transcellular Membrane Diffusion



Dahlgren & Lennernäs
Book Chapter 2021

Small intestinal barrier

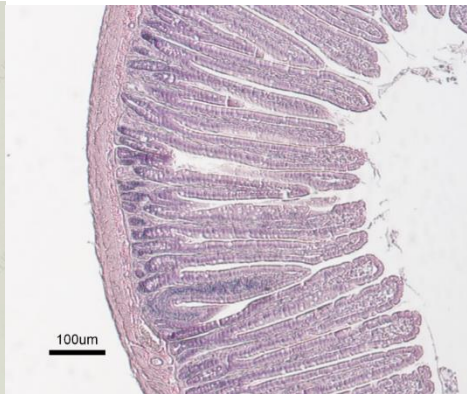
- Is organized in finger-like protrusions called villi and invaginations called crypts.
- Is a dynamic physiological barrier that is sensing and receiving feedback neuroendocrine signals that maintains the delicate balance between permeability and protective barrier functions



Small and Large Intestinal Mucosa and site of measurements



UPPSALA
UNIVERSITET

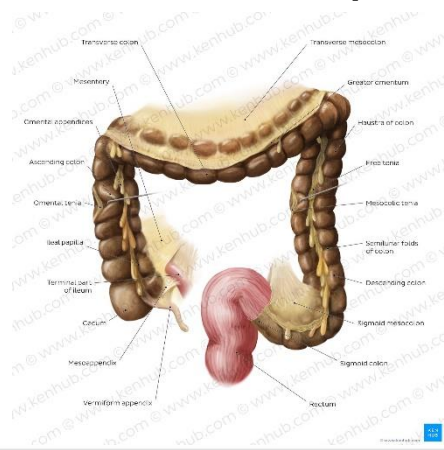


- Enterocytes
- Goblet cells
- Enteroendocrine cells
- Paneth cells



Colon mucosa is lined by simple columnar epithelium (lamina epithelialis) with long microvilli.

<https://www.sciencephoto.com/media/309980/view/artwork-of-a-section-through-an-intestinal-villus>

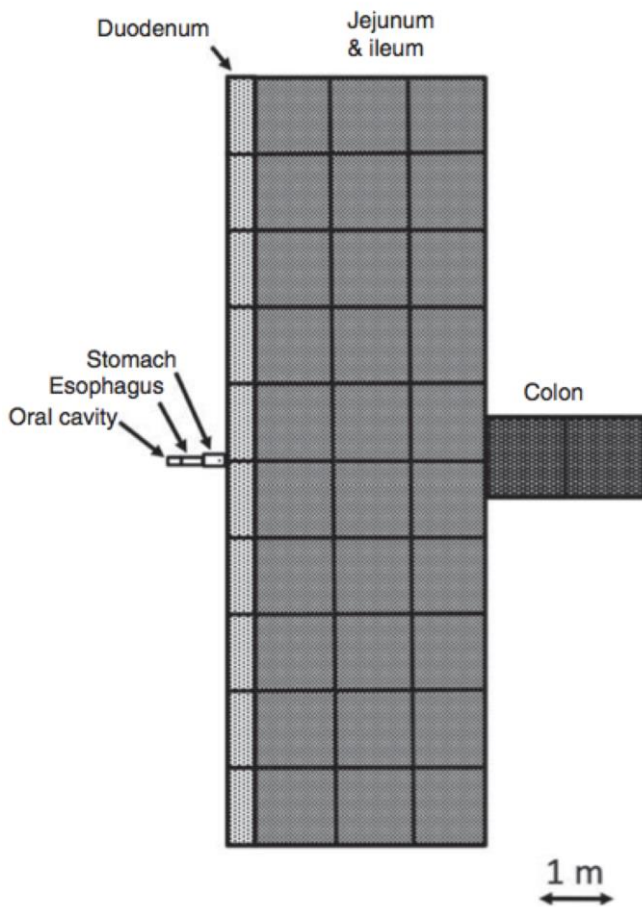


The colon makes up the longest part of the large intestine. It begins from the caecum at the ileocecal valve and ends in the rectum.

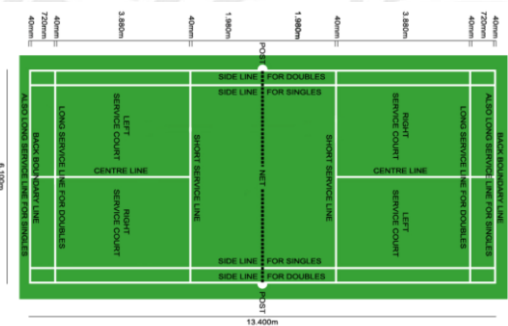
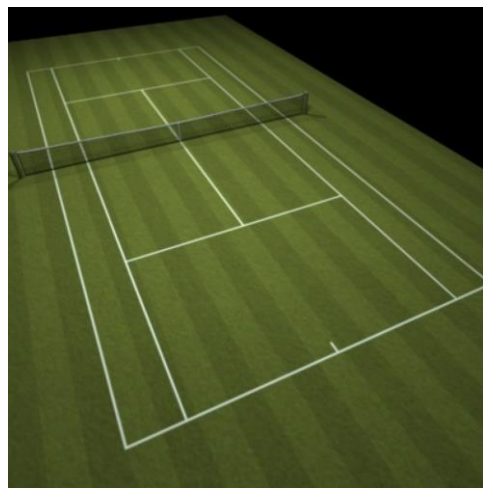
Approximate anatomical distribution of the mucosal luminal surfaces along the digestive tract.



Villi



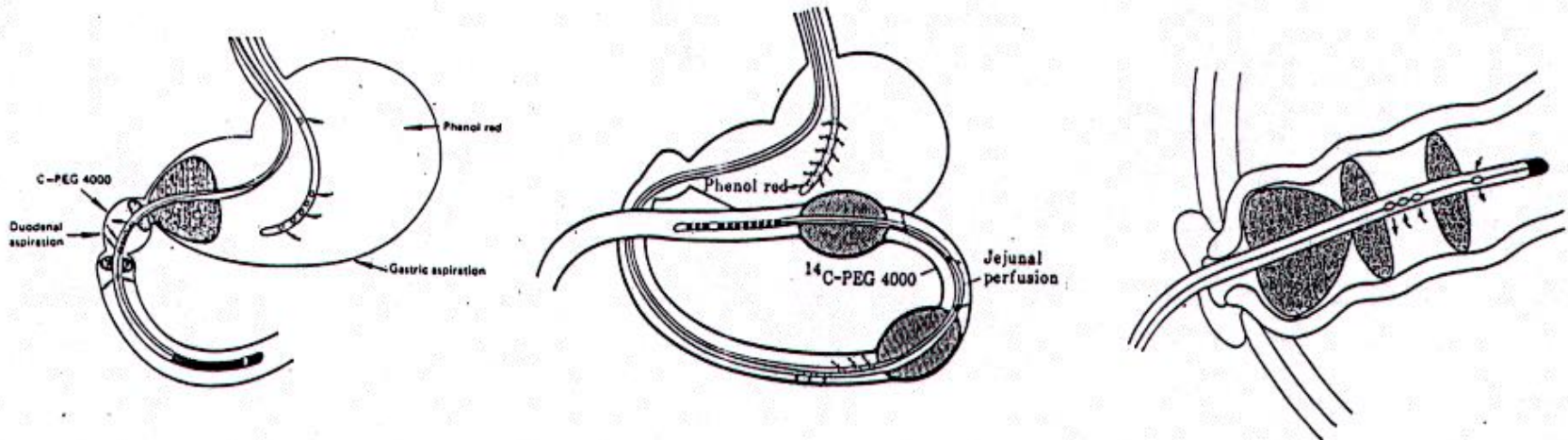
- Approximately the area (A) used to calculate P_{eff} is 0.33 m^2 in the perfused jejunal segment (LOC-I-GUT)
- According to novel data the total A of the GI mucosa in adult humans is calculated to be about $30\text{-}40 \text{ m}^2$.
- “The total area of the human adult gut mucosa is not in the order of tennis lawn ($300\text{-}400 \text{ m}^2$), rather is that of half a badminton court ($30\text{-}40 \text{ m}^2$)”.



Helander HF & Fändriks L. Scand. J Gastroenterology. 2014; 49: 681–689
Surface area of the digestive tract – revisited

In vivo single-pass perfusion of jejunum and rectum in humans

The Loc-I-GUT Concept



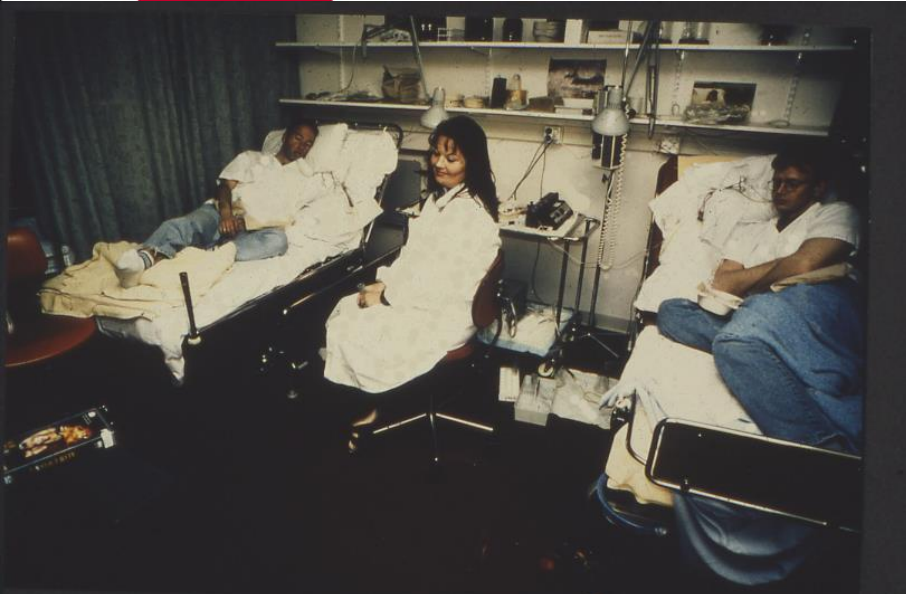
Knutson L., Odling B. and Hällgren R. A new technique for segmental jejunal perfusion in man. *Am. J. Gastroenterol.* 84: 1278-1284, 1989.

Lennernäs H., Ahrenstedt Ö., Hällgren R., Knutson L., Ryde M. and Paalzow L.K. Regional jejunal perfusion, a new *in vivo* approach to study oral drug absorption in man. *Pharm. Res.* 9, 1243-1251, 1992.

Clinical experiments performed *in vivo* in humans: Loc-I-Gut



Knutson T, Fridblom P, Ahlström H, Magnusson A, Tannergren C, Lennernäs H. Mol Pharm. 2009;6(1):2-10



The perfused jejunal segment in humans with Loc-I-Gut®

(Knutson T, Knutson L. and Lennernäs H.)



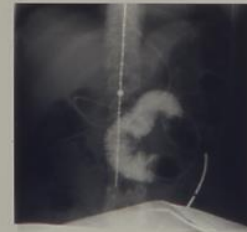
Male



Male



Male



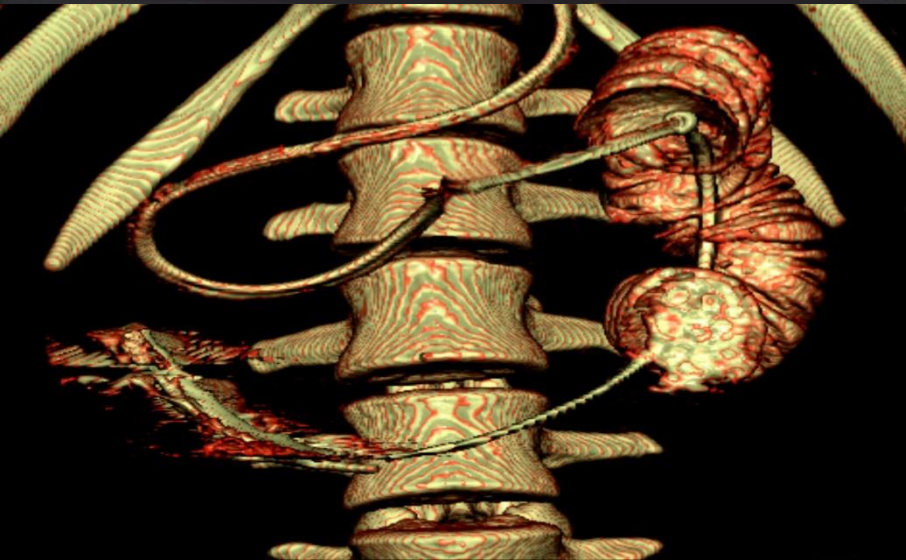
Female



Female



Female

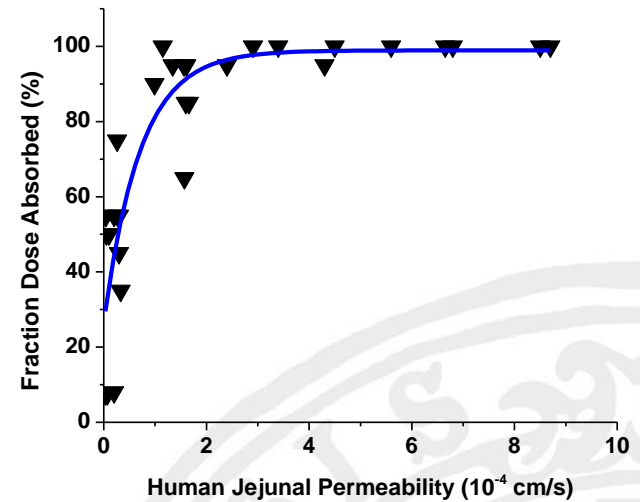
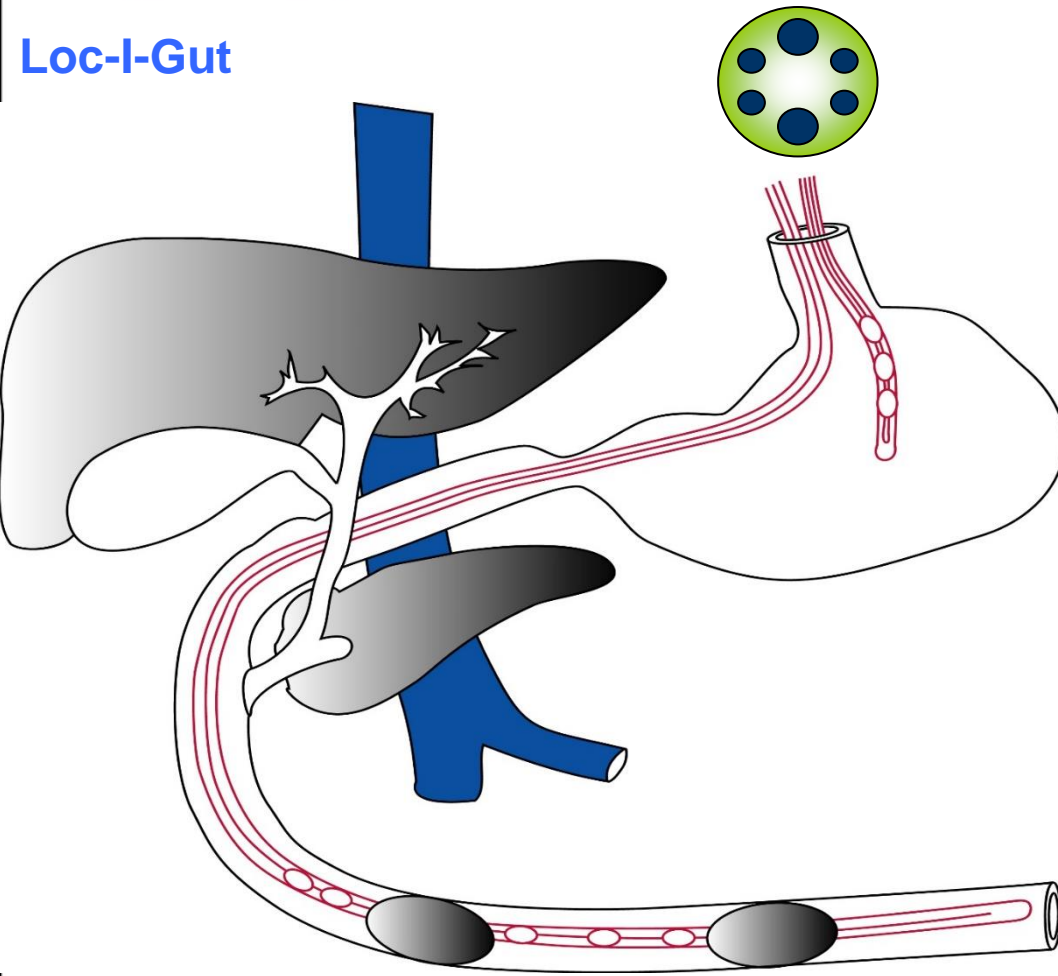


With Multi-slice Computed Spiral Tomography and air as a contrast medium a three dimensional view of the perfused segment is obtained.

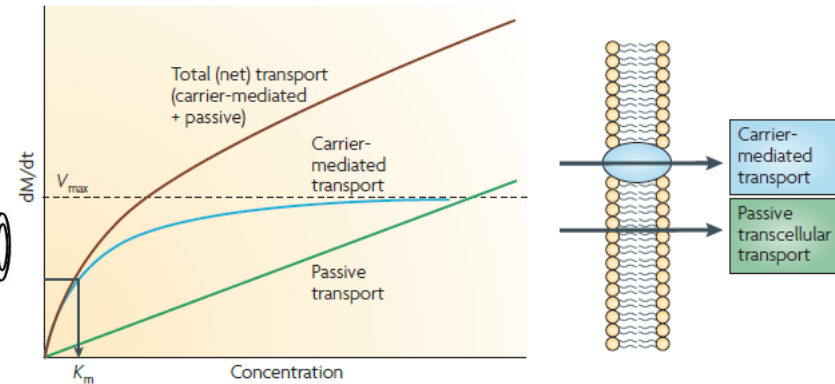
Intestinal permeability and plasma pharmacokinetic assessment simultaneously in humans (in vivo)

Lennernäs H. et al, Pharm Res, 1992, 9(10), 1243-1251

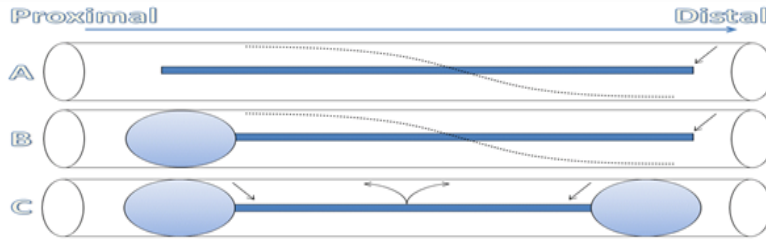
Loc-I-Gut



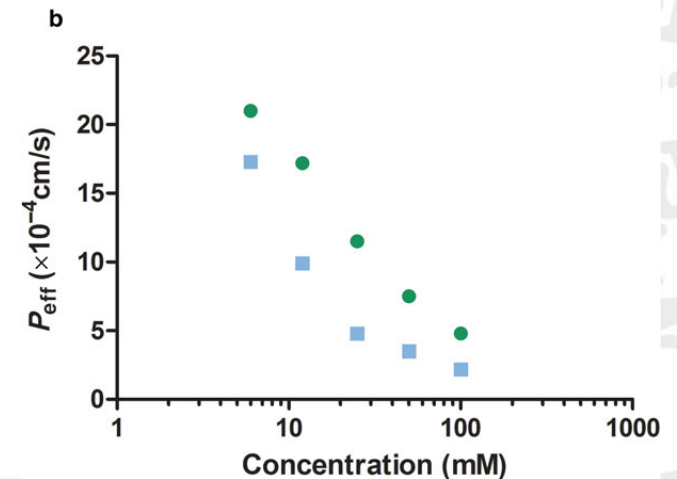
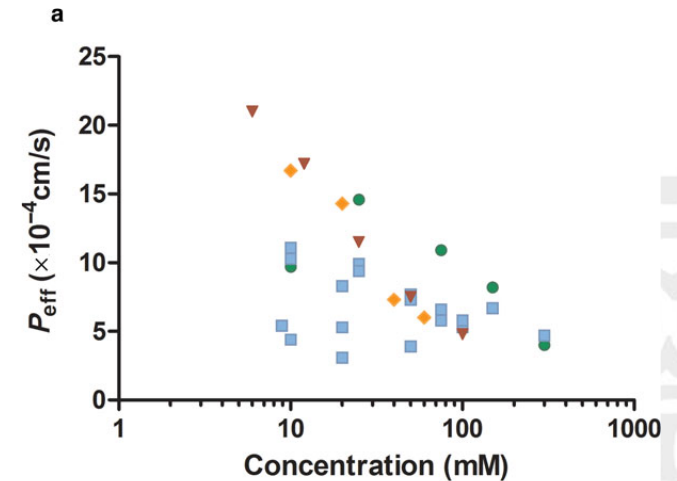
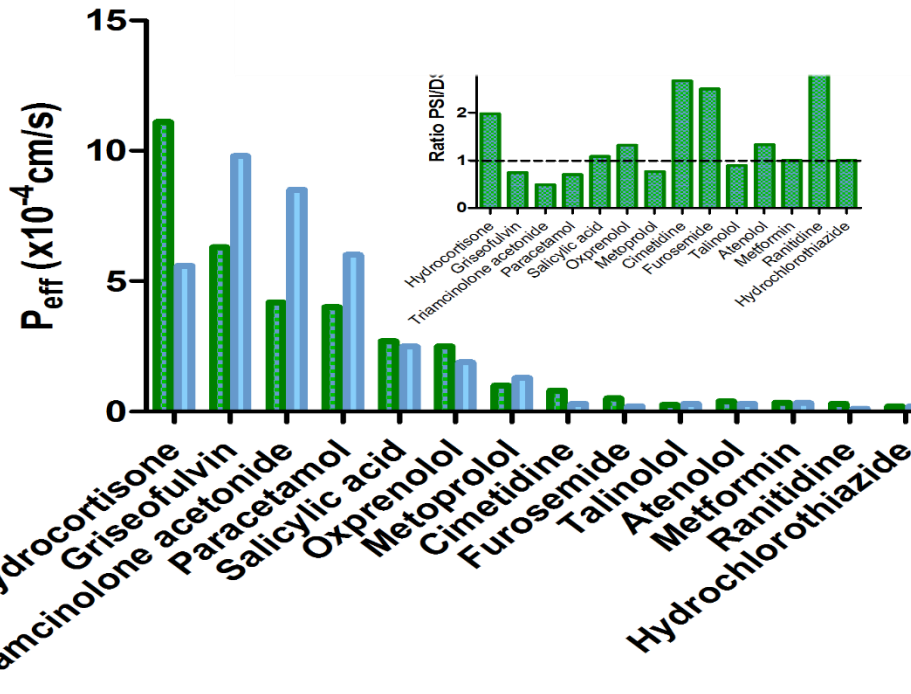
(Lennernäs. Xenobiotica 1992-2007)



Proximal (PSI) (green) and distal (DSI) (blue) small intestinal *in vivo* permeation (P_{eff}) and regional P_{eff} ratio of 14 model compounds determined using open intestinal perfusion.



Schematic presentation (right) of the clinical intestinal perfusion models, A – The open perfusion system, B – The proximal balloon perfusion system, C - The double balloon perfusion system.



Human study

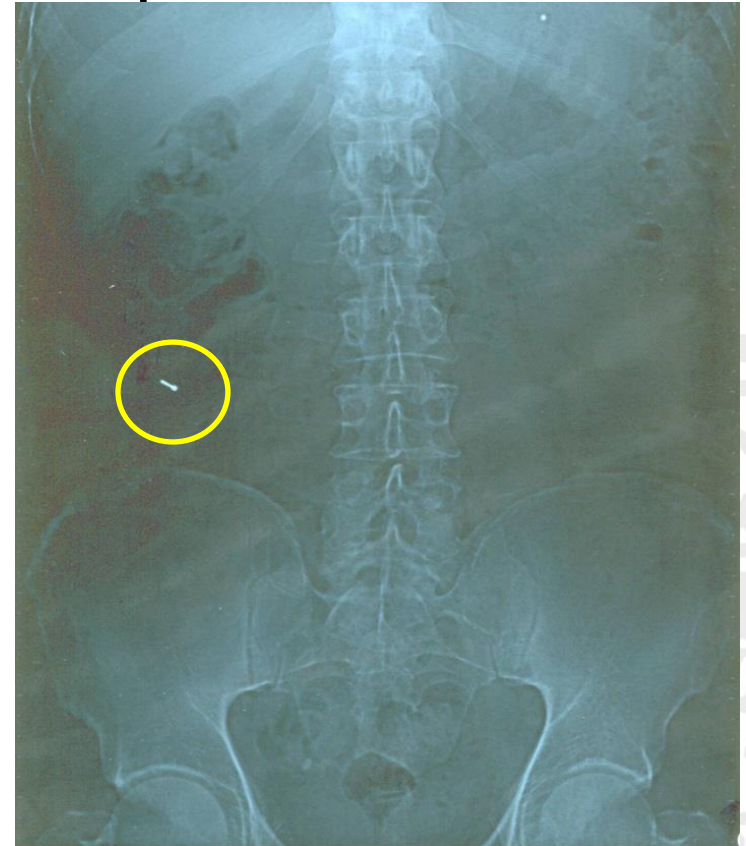
The Bioperm tube-capsule



Diameter
0.6 mm

Size
30 * 10 mm

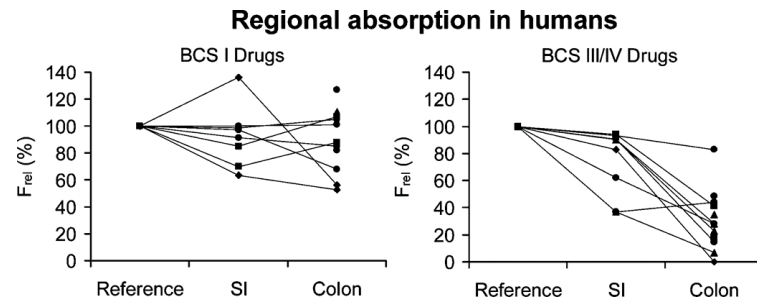
- Capsule positioning verified using:
 - Tube length
 - Jejunum 1 m
 - Ileum 2.5 m
 - Colon 3.5-4 m
 - X-ray (fluoroscopy)



1. Petri N, Borga O, Nyberg L, Hedeland M, Bondesson U, Lennernas H. *Int J Clin Pharmacol Ther.* 2006 Feb;44(2):71-9.
2. Dahlgren D, Roos C, Lundqvist A, Abrahamsson B, Tannergren C, Hellström PM, Sjögren E, Lennernas H. *Regional Intestinal Permeability of Three Model Drugs in Human.* *Mol Pharm.* 2016 Sep 6;13(9):3013-21.

Human study

Regional intestinal permeability



Tannergren C, Bergendal A, Lennernäs H, Abrahamsson B. Toward an increased understanding of the barriers to colonic drug absorption in humans: implications for early controlled release candidate assessment. *Mol Pharm.* 2009 Jan-Feb;6(1):60-73.

Aim

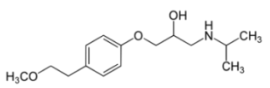
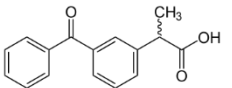
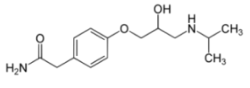
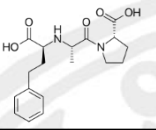
- To determine reference regional intestinal permeability values of three model drugs in human

Method

- Cassette dosing of **atenolol**, **metoprolol** and **ketoprofen** in solution.
- 14 volunteers
- Dosed on 4 occasions
 - 1 x intravenously (1 ml)
 - 3 x intraluminally (13 ml) – jejunum, ileum and colon
- Blood samples collected following the administrations
- Individual P_{eff} calculated using the Deconvolution P_{eff} model



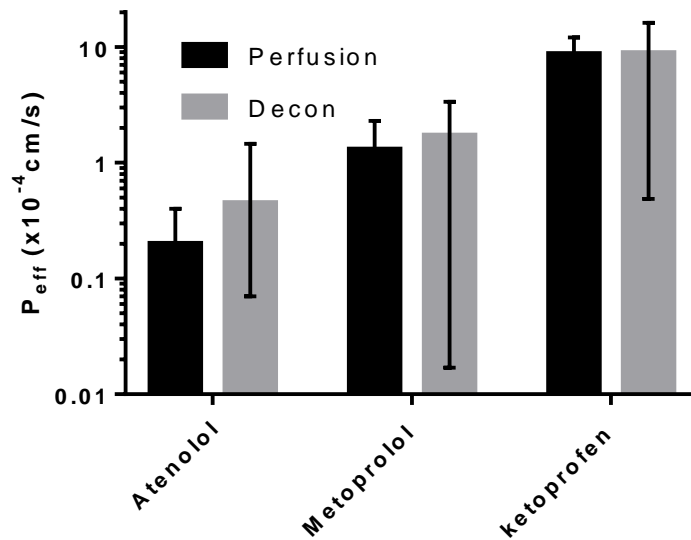
Model drugs

	Model drugs			
	Human study			
	Rat and dog studies			
	Metoprolol	Ketoprofen	Atenolol	Enalaprilat
BCS Class	I	II	III	III
Structure				
MW (g/mol)	267	254	266	348
pKa	9.6 – base	3.88 - acid	9.6 – base	3.17 - base 7.84 - acid
Log P	2.07	3.37	0.18	-0.13
Log D pH 7.4	0	0.1	-2	-1.0
Log D pH 6.5	-0.5	0.8	<-2	-1.0
PSA	57.8	54.2	88.1	102.1
HBA/HBD	4/2	3/1	4/4	6/3

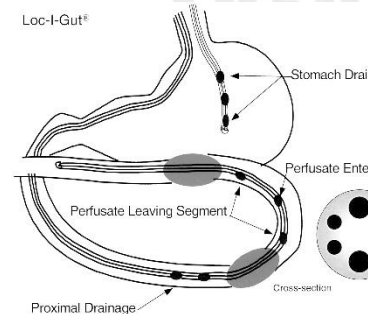
Human study

Effective jejunal permeability (P_{eff})

		Atenolol	Metoprolol	Ketoprofen	
P_{eff} ($\times 10^{-4}$ cm/s)	Deconvolution	0.45 (0.07-1.46)	1.72 (0.016-3.38)	8.85 (0.49-16.14)	median (range)
	Perfusion	0.2 (0.2)	1.3 (1.0)	8.7 (3.4)	mean (SD)

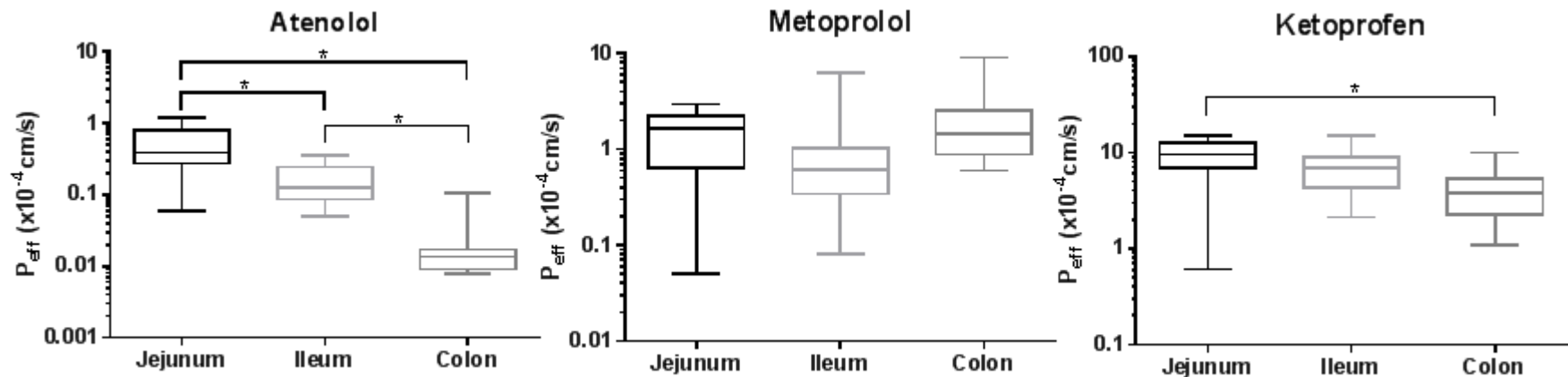


VS.



Human study

Regional effective intestinal permeability (P_{eff})



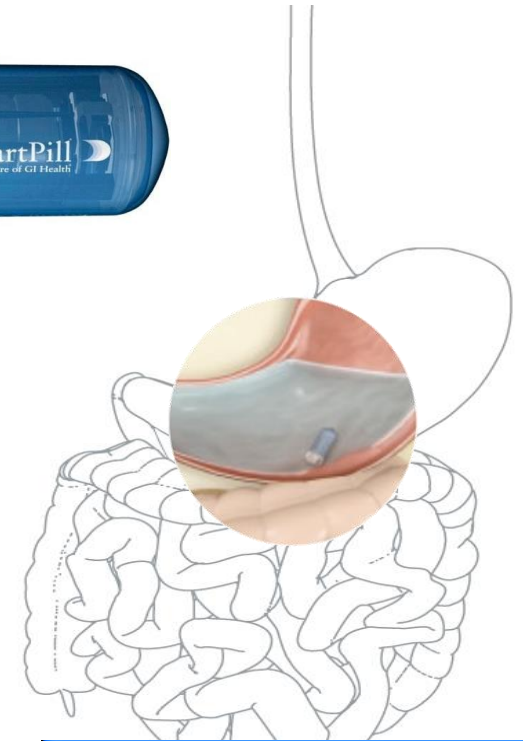
	Atenolol	Metoprolol	Ketoprofen
P_{eff} ($\times 10^{-4}$ cm/s)			
Jejunum	0.45 (0.07-1.46)	1.72 (0.016-3.38)	8.85 (0.49-16.14)
Ileum	0.15 (0.06-0.42)	0.72 (0.09-7.53)	6.53 (1.49-10.44)
Colon	0.013 (0.01-0.10)	1.30 (0.54-7.74)	3.37 (0.98-9.07)
Median (range)			

SmartPill capsule motility procedure and future devices

- Measures pressure, pH and temperature throughout the GI tract.

These measurements are used to:

- Determine gastric emptying time
- Determine combined small/large bowel transit time
- Intraluminal pH
- Determine whole gut transit time
- Characterize pressure patterns and provide motility indices for the antrum and duodenum
- To dose and calculate regional intestinal permeability/absorption (depend on availability of IV dosing)



Test Summary

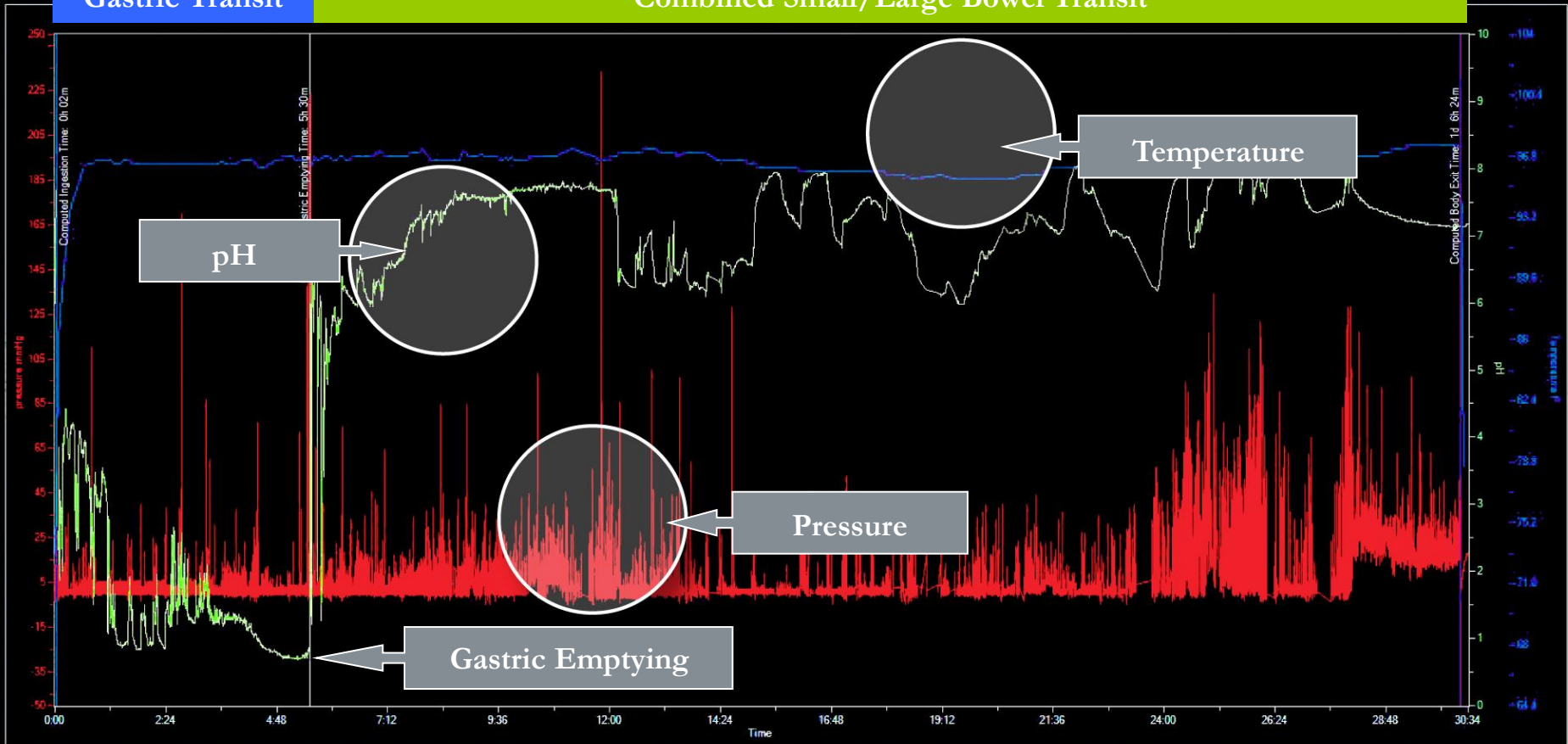
Clinical Data		Descriptive Data	
Patient Information			
Patient Name	ID	None-002016	Test Date
			6/16/2005
Event Times			
	Physician Determined	Elapsed Time	Computed
	Clock Time		Clock Time
Capsule Ingested at:	n/a	n/a	6/16/05 09:36 AM
			0:51
Capsule Left Stomach at:	n/a	n/a	6/16/05 11:51 AM
			3:06
Capsule Left Body at:	n/a	n/a	6/17/05 16:09 PM
			31:24
Transit Times (hr:min)			
Physician Determined Transit Times		Computed Transit Times	
Gastric Emptying Time	n/a	Gastric Emptying Time (diagnostic cutoff at 4 hrs)	3:06
Small/Large Bowel Transit Time	n/a	Small/Large Bowel Transit Time	28:18
Total GI Transit Time	n/a	Total GI Transit Time (normal male: 28hr-24min) (normal female: 35hrs-24min)	31:24
Gastric pH Values			
High	30.8		
Low	0.8		

Close

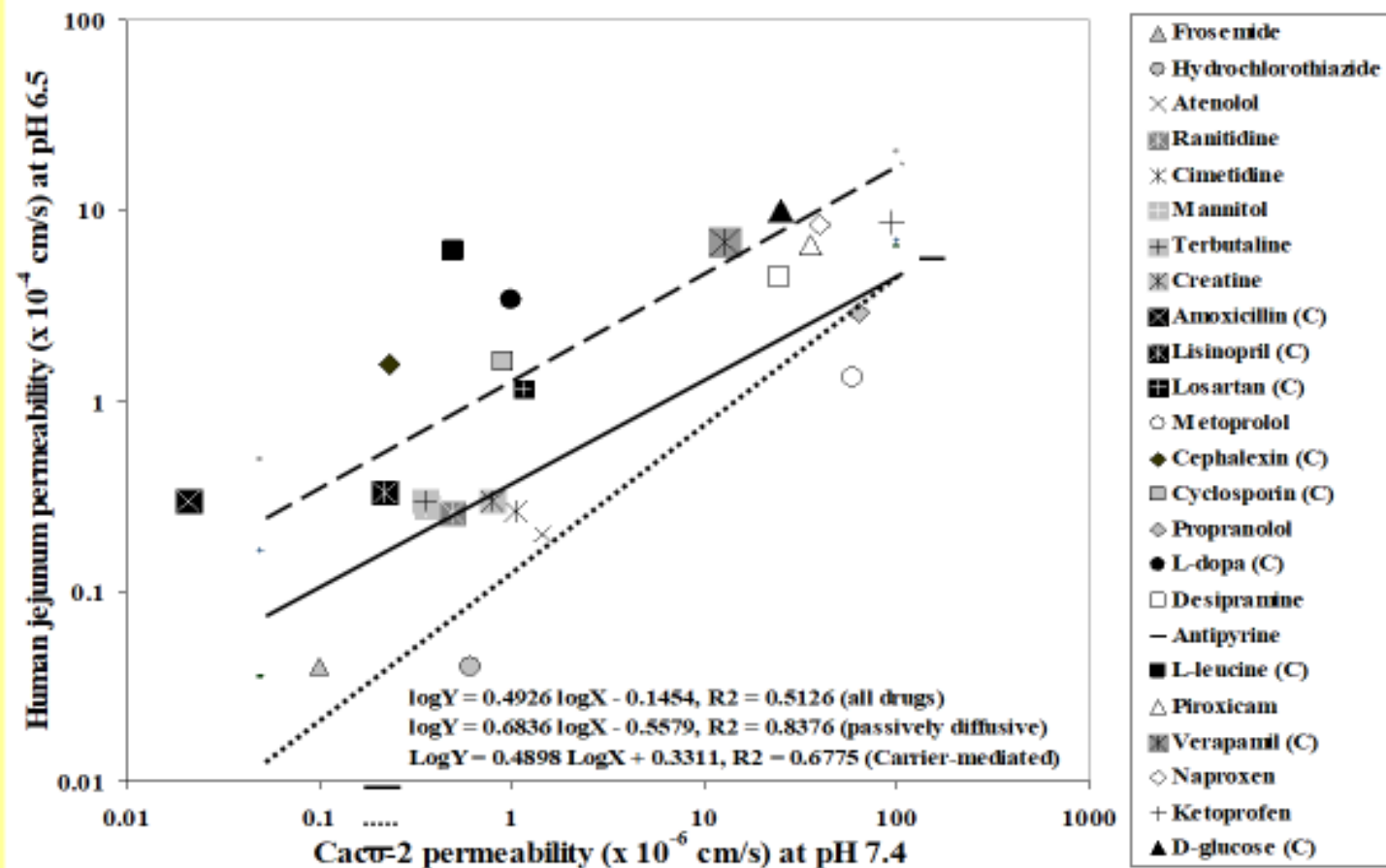
SmartPill – GI-transit, motility, intraluminal pressure and pH

Gastric Transit

Combined Small/Large Bowel Transit



Human jejunal Permeability vs human colorectal adenocarcinoma (Caco-2) first isolated in 1977 from a 72-year-old Caucasian male)

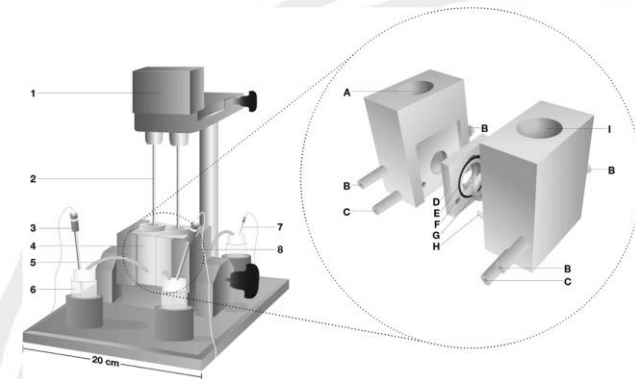
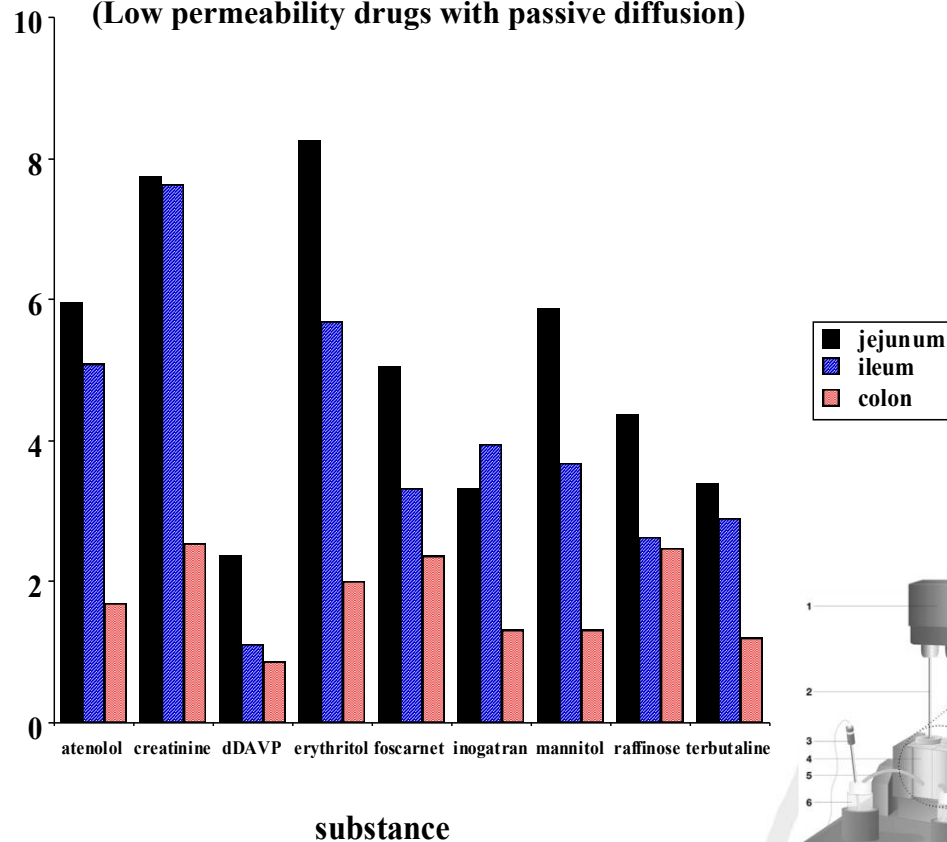




Regional Intestinal Permeability in Rat (10-6, cm/s)

Apparent permeabilities in various intestinal regions in rats.

(Low permeability drugs with passive diffusion)



Cholesterol, sphingolipids, and glycolipids, constituents in the cell membrane that modulate its properties, and subsequently the permeability to drugs. In particular, membranes containing cholesterol exhibit greater acyl-chain order and increased stiffness, reflected in a smaller average area per lipid, and, hence, a reduced permeability to substrates.

Sjöberg Å, Lutz M, Tannergren C, Wingolf C, Borde A, Ungell AL. Comprehensive study on regional **human** intestinal permeability and prediction of fraction absorbed of drugs using the Ussing chamber technique. Eur J Pharm Sci. 2013 Jan 23;48(1-2):166-80.

Table 2

Apparent permeability (P_{app}) for compounds in human intestinal tissue in the modified Ussing chamber. Results are presented as mean \pm SD ($n=x$). Numbers indicate the compounds used in the jejunum correlation curve and letters indicate the compounds for colonic correlation curve.

Comp. No.	Compound	Apparent permeability, P_{app} [$\times 10^{-6}$ cm/s] (mucosa to serosa direction)					
		Fa (%) p.o.*	Fa (%) i.c.**	Duodenum	Jejunum	Ileum	Colon
1	Sulphasalazine	12			0.09 \pm 0.06 (2)		
A	Fexofenadine		13				0.22 \pm 0.08 (4)
B	Ranitidine		9				0.62 \pm 0.29 (4)
2	Vinblastine	25			1.31 \pm 2.14 (4)		
3,C	Digoxin	81	66		1.44 \pm 0.72 (7)		2.83 \pm 1.26 (4)
4,D	Melagatran	6	3		1.51 \pm 0.39 (3)		1.20 \pm 1.07 (2)
5,E	Ximelagatran	45	39	3.15 \pm 0.07 (2)	3.03 \pm 1.08 (5)	1.01 (1)	1.90 \pm 0.66 (4)
6	Quinidine	80			3.36 \pm 0.56 (5)		
7	Cimetidine	64			3.74 \pm 0.47 (5)		
8,F	Atenolol	56	28	2.61 (1)	4.11 \pm 1.32 (4)		1.27 \pm 0.64 (5)
9	Oseltamivir	81			4.64 \pm 1.17 (2)		
10	Mannitol	38		4.85 \pm 0.86 (5)	5.56 \pm 2.01 (253)	1.39 \pm 0.56 (3)	1.22 \pm 0.79 (104)
11	Rosuvastatin	50			6.95 \pm 1.05 (3)		1.07 \pm 0.25 (2)
12	Diclofenac	99			8.55 \pm 0.19 (2)		
13,G	Oxprenolol	90	74		9.50 \pm 1.73 (2)		30.4 \pm 8.6 (4)
14,H	Metoprolol	95	100		15.9 \pm 3.69 (4)		18.8 \pm 4.00 (3)
15	Creatinine	100		4.24 (1)	20.2 \pm 7.84 (4)		2.55 \pm 2.74 (3)
16	Hydrocortisone	89		13.5 \pm 5.45 (3)	22.3 \pm 4.22 (4)		15.0 \pm 6.49 (4)
I	Diltiazem		82				23.6 \pm 2.3 (3)
17	Propranolol	95		18.0 \pm 6.72 (4)	31.9 \pm 17.0 (24)	22.4 \pm 14.6 (5)	35.4 \pm 14.2 (7)
18	Verapamil	100			36.0 \pm 10.0 (4)		
19	Midazolam	100			38.0 \pm 16.0 (2)		
20,J	Salicylic acid	100	100	18.4 (1)	41.1 \pm 16.5 (4)		13.3 \pm 3.11 (2)
21	Indomethacine	100			48.2 \pm 12.4 (4)		
22	Antipyrine	100		26.3 \pm 6.99 (3)	49.7 \pm 13.3 (4)		54.6 \pm 13.0 (3)
23	Testosterone	100			68.0 \pm 10.9 (6)		
24	D-Glucose	100			113 \pm 49.4 (29)		1.02 \pm 0.52 (4)
25	L-Leucine	100			140 \pm 40.8 (4)		2.63 \pm 0.86 (3)

P_{app} for some of the compounds has been presented in the paper by Ungell (2002).

* Fraction absorbed data obtained from references: Galetin and Houston, 2006; Tannergren et al., 2009; Thelen et al., 2011; Ungell, 2002; Ungell and Karlsson, 2003. In house data for ximelagatran and rosuvastatin.

** Fraction absorbed data obtained from reference: Tannergren et al., 2009.



Experimental Determination of the Membrane Permeability in different types of assays to provide estimates of the apparent membrane permeability

Chipot C. Predictions from First-Principles of Membrane Permeability to Small Molecules: How Useful Are They in Practice? *J Chem Inf Model.* 2023 Aug 14;63(15):4533-4544.

pubs.acs.org/jcim

Perspective

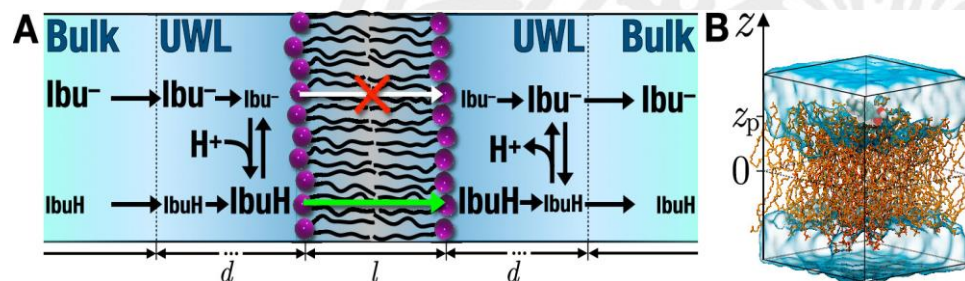
Table 1. Apparent Membrane Permeability (P_{app}) of Ibuprofen Measured Using a Variety of Methods, from In Vitro Artificial Membrane Assays to In Vivo Animal Intestinal Perfusion

Assay	P_{app} (cm/s)	reference
Caco-2	52.5×10^{-6}	
PAMPA (pH 5.5)	10.8×10^{-6}	21
PAMPA (pH 7.4)	6.8×10^{-6}	
Caco-2	30.1×10^{-6}	22
rat intestinal	200×10^{-6}	23
solution-based PAMPA	10.8×10^{-6}	
trilayer PAMPA	6.8×10^{-6}	24
phospholipid vesicle (pH 6.2)	13.3×10^{-6}	
phospholipid vesicle (pH 7.4)	8.4×10^{-6}	25
vinblastine-treated Caco-2	76.2×10^{-6}	
MDCK-MDR1 ^a	74.3×10^{-6}	26
jejunum	228×10^{-6}	
middle small intestine	205×10^{-6}	27
ileum	206×10^{-6}	
Permeapad ²⁸	16.6×10^{-6}	29

^aMDCK cells with the MDR1 gene encoding for efflux P-glycoprotein.

The apparent membrane permeability, P_{app} , depends on the nature of the cell-line assay, and applied conditions of the experiment, and will vary from batch to batch.

Which membrane model would provide the most accurate and precise representation of the permeability assays. How can these values be used theoretical of P_m in drug discovery as well as PBBM.



How useful are membrane-permeability estimates from computer based molecular dynamics simulations by using the inhomogeneous solubility–diffusion model ?

The gastrointestinal tract plays a central role in the maintenance of homeostasis in the body through endocrine and immune functions as well as digestive functions. Gastrointestinal-released hormones and an interplay with neurosignaling play a significant role in these processes.

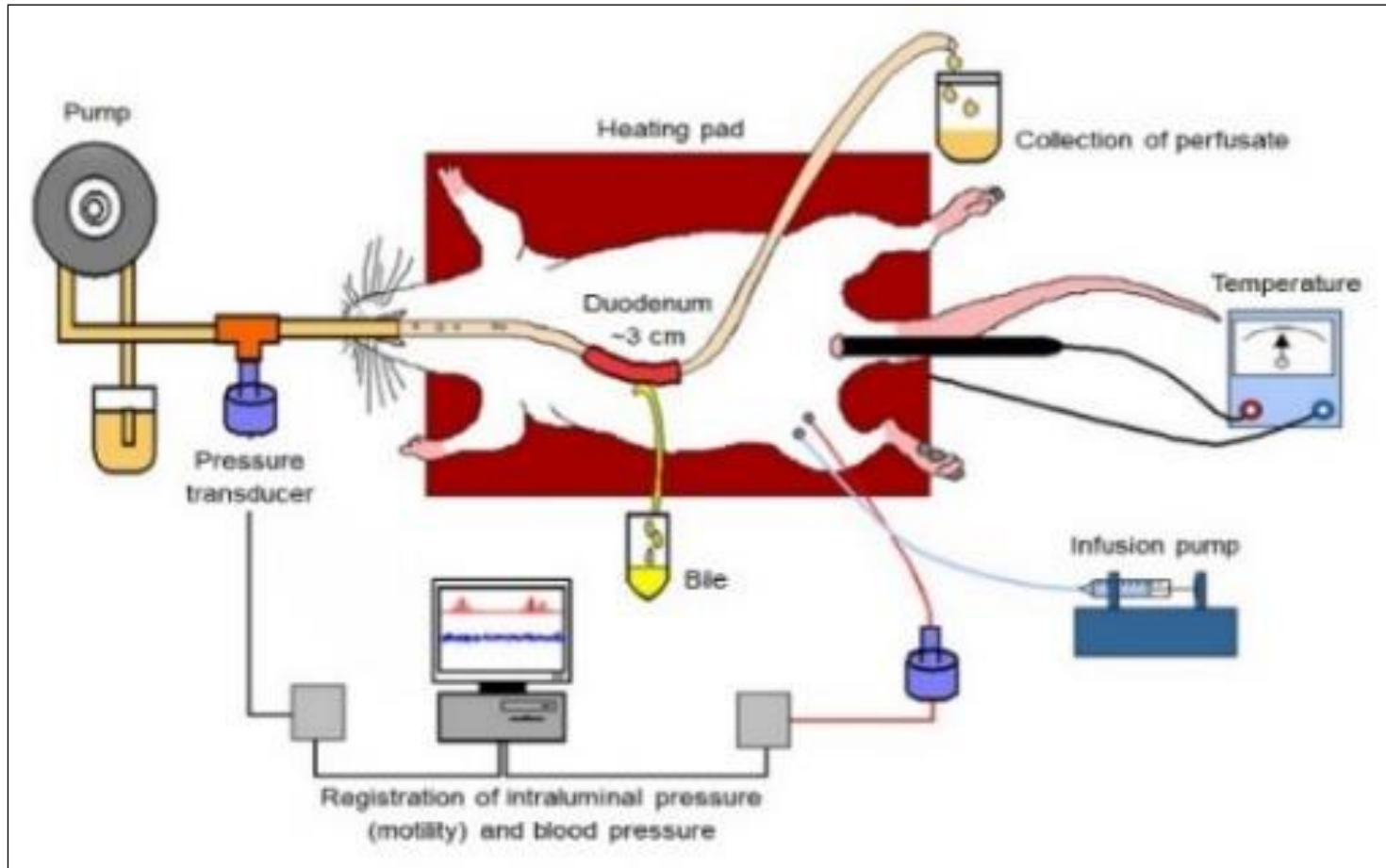


Figure 2. Schematic illustration of the in vivo rat single-pass intestinal perfusion (SPIP) model, allowing continuous monitoring intestinal epithelial permeability, metabolism, motility, ion transport, fluid flux and systemic blood pressure.

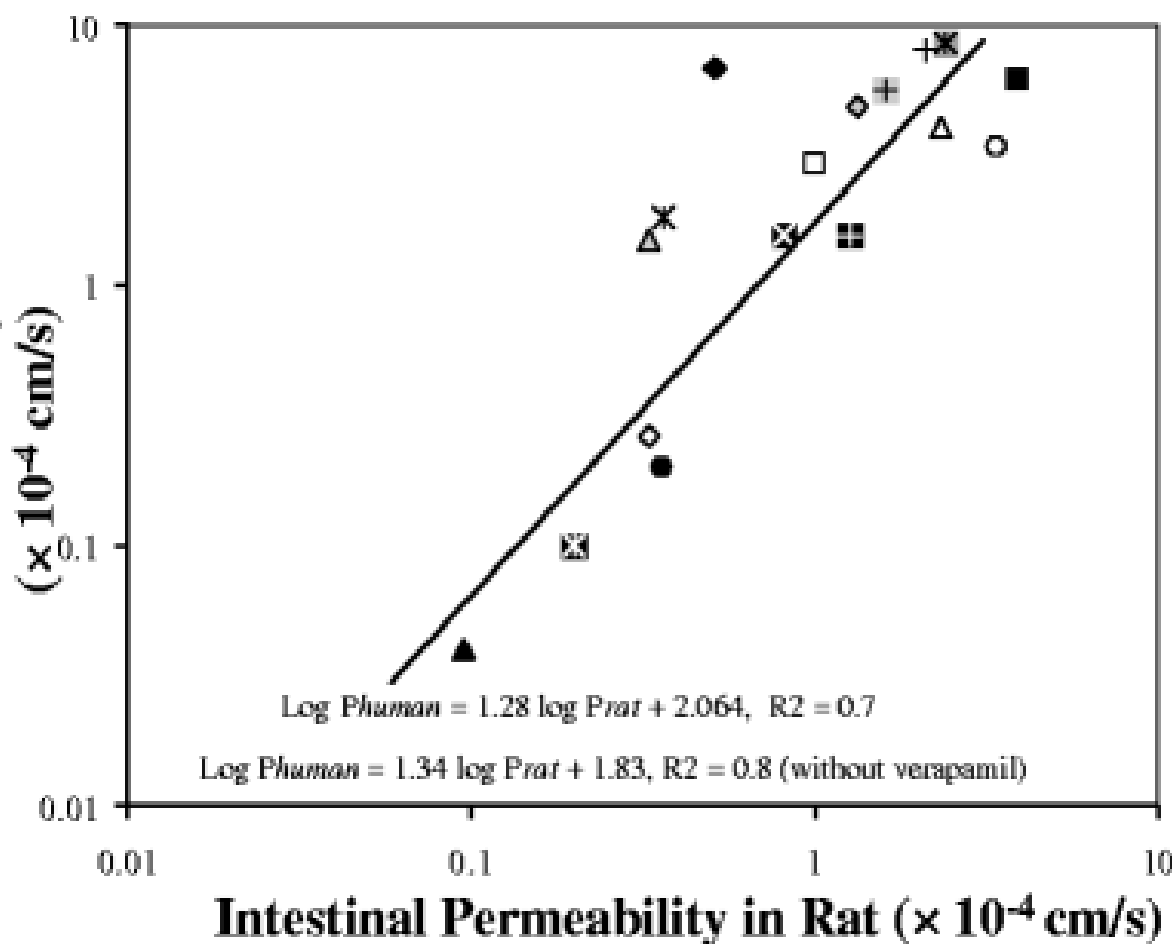
Correlation of oral permeability between rat and human

Why is it Challenging to Predict Intestinal Drug Absorption and Oral Bioavailability in Human Using Rat Model

Xianhua Cao, Seth T. Gibbs, Lanyan Fang, Heather A. Miller, Christopher P. Landowski, Ho-Chul Shin, Hans Lennernas, Yanqiang Zhong, Gordon L. Amidon, Lawrence X. Yu and Duxin Sun
Pharm Res. 2006 23(8):1675-86.



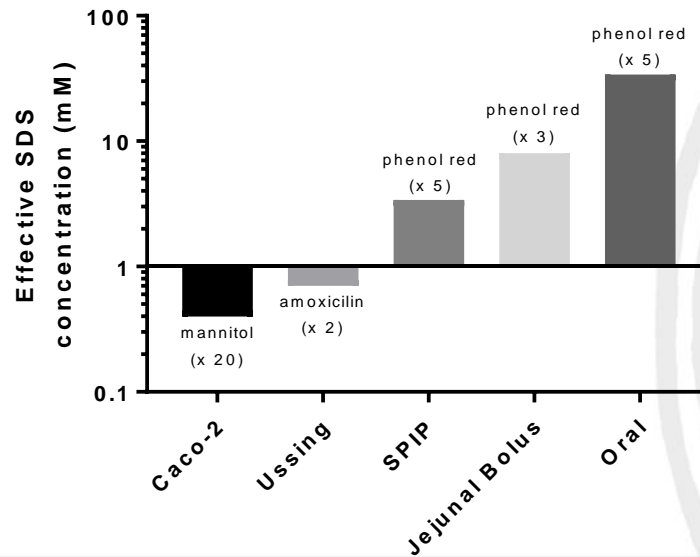
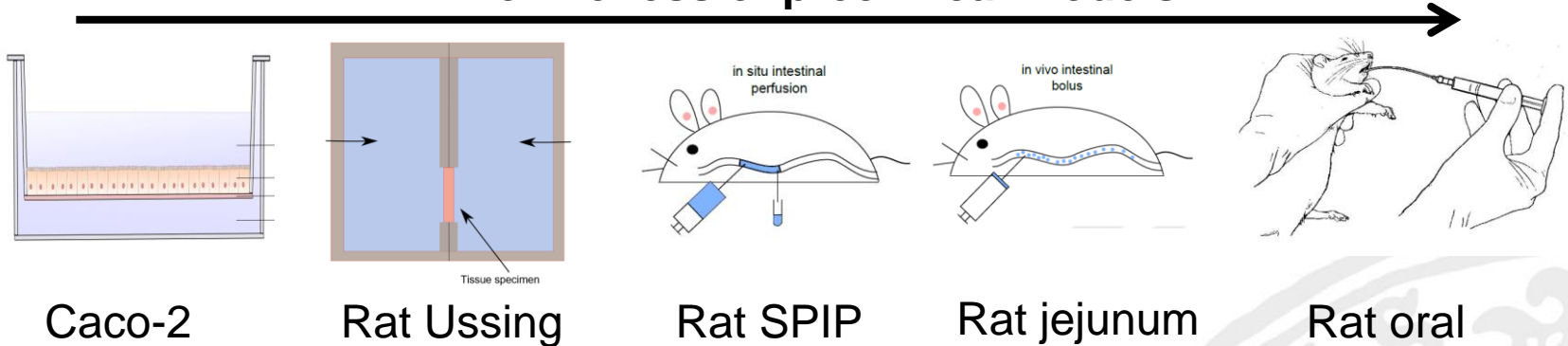
Intestinal Permeability in Human



- ◆ Verapamil
- Leucine
- △ Phenylalanine
- L-Dopa
- × Valacyclovir
- ⊠ Enalapril
- ⊞ Cephalixin
- ⊞ Methyldopa
- Propranolol
- ◇ Cimetidine
- Atenolol
- ▲ Furosemide
- ⊠ Ketoprofen
- + Naproxen
- ⊞ Antipyrine
- △ Metoprolol
- ◇ Tacrolimus

The model is important! (effect of excipients)

In vivo likeness of preclinical models

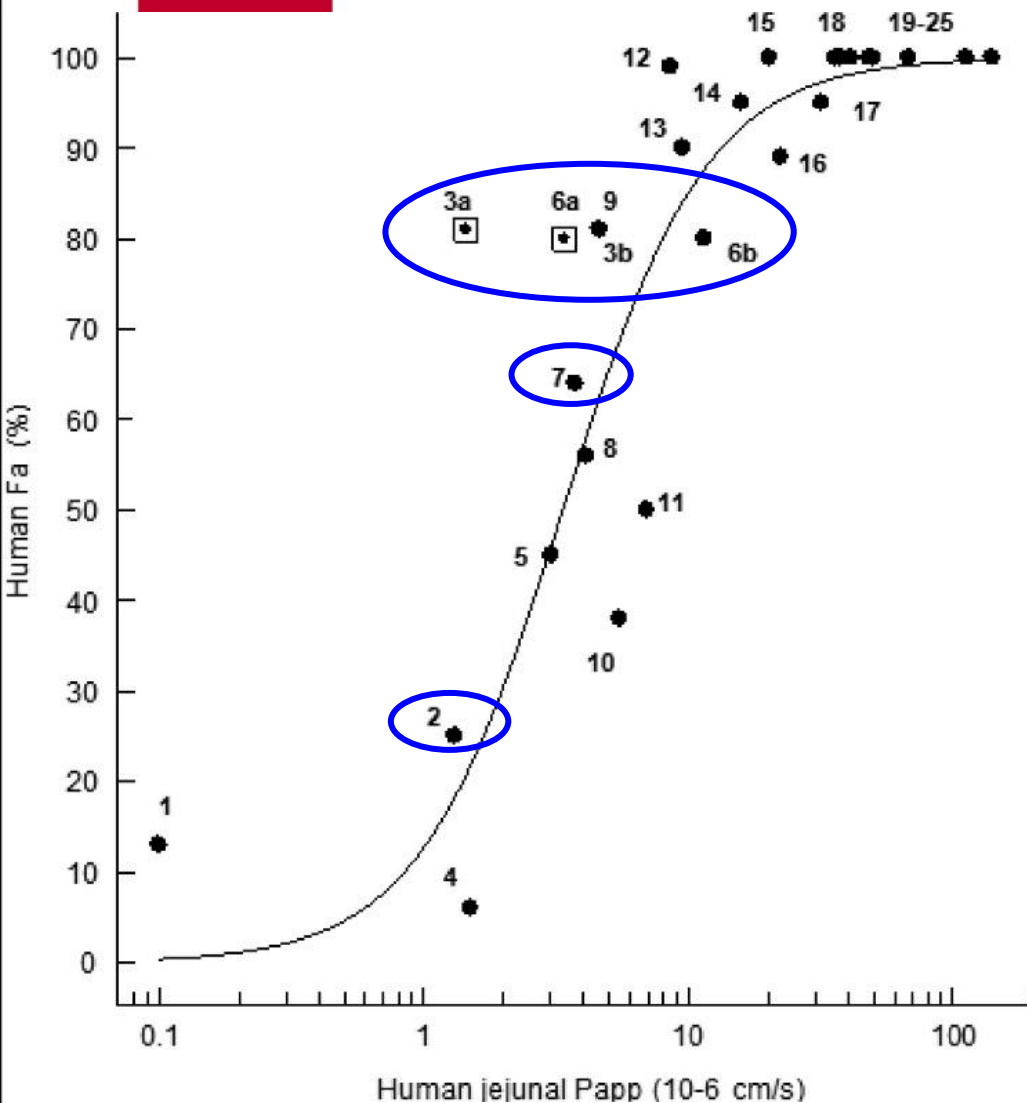


Dahlgren D, Lennernäs H. Intestinal Permeability and Drug Absorption: Predictive Experimental, Computational and In Vivo Approaches. *Pharmaceutics*. 2019 Aug 13;11(8):411.

Bidirectional permeability to assess uptake or **efflux**

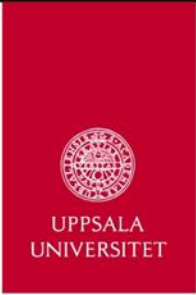


UPPSALA
UNIVERSITET

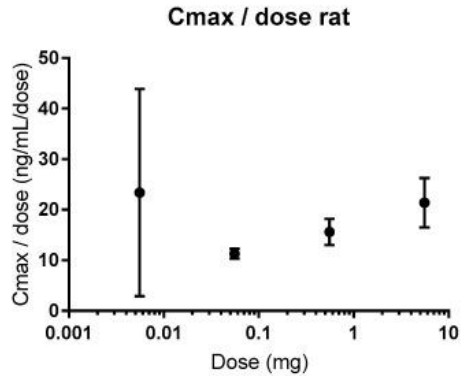
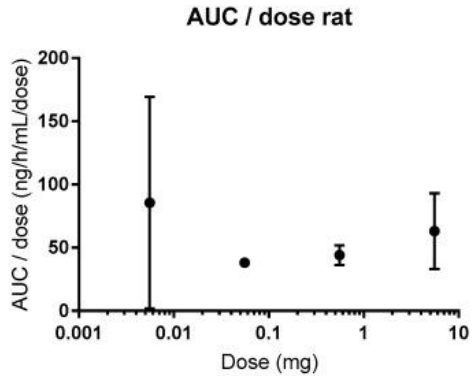
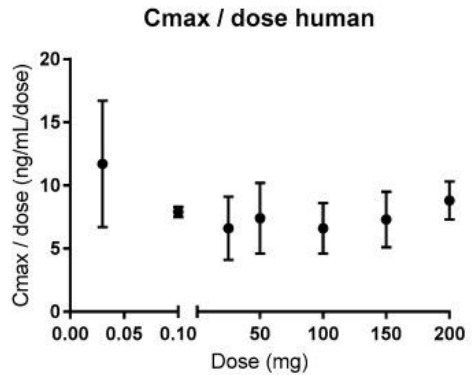
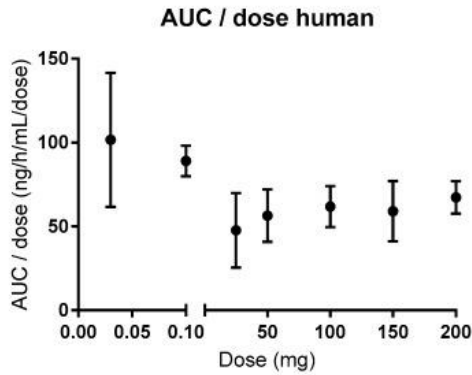


Efflux ratio in this study for vinblastine (2), digoxin (3a,3b), cimetidine (7) and quinidine (6a,6b) were ER = 4.25, 5.41, 1.79 and 5.85

Sjöberg Å, Lutz M, Tannergren C, Wingolf C, Borde A, Ungell AL. Comprehensive study on regional human intestinal permeability and prediction of fraction absorbed of drugs using the Ussing chamber technique. *Eur J Pharm Sci.* 2013 Jan 23;48(1-2):166-80.



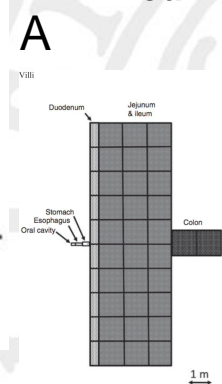
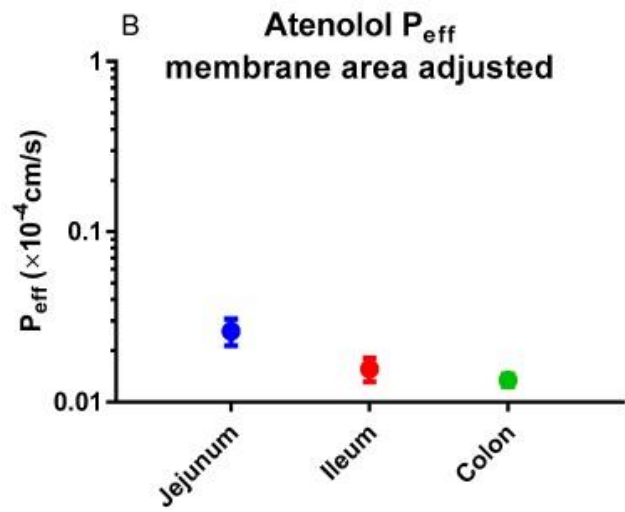
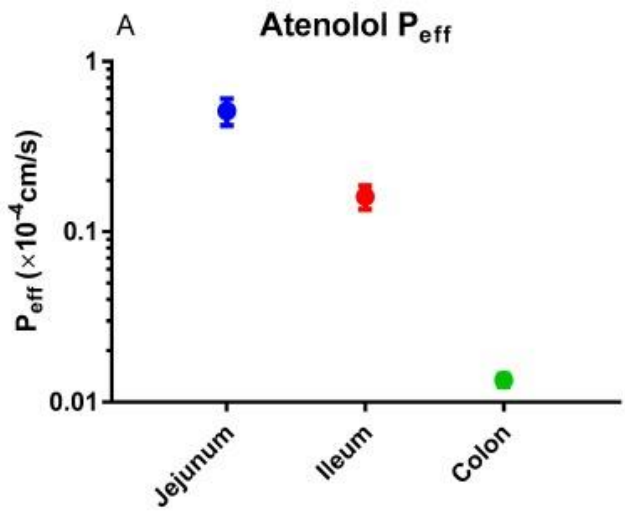
Dahlgren D, Lennernäs H. Intestinal Permeability and Drug Absorption: Predictive Experimental, Computational and In Vivo Approaches. *Pharmaceutics*. 2019 Aug 13;11(8):411.



Dose proportionality in the AUC and Cmax of atenolol in humans (0.1–200 mg) and rats (0.55 µg–5.5 mg).

Efflux ratio for atenolol in Caco-2 model range from 0.18-3.8

(A) Regional intestinal effective permeability (P_{eff}) of atenolol in humans. (B) Surface area (villi and folds)-adjusted regional intestinal P_{eff} values for atenolol in humans: jejunum 19-fold, ileum 10-fold, colon 1-fold



Colonic membranes containing cholesterol exhibit greater acyl-chain order and increased stiffness, and hence a reduced permeability to substrates.

Trends in Molecular Properties, Bioavailability, and Permeability across the Bayer Compound Collection (O'Donovan et al.)

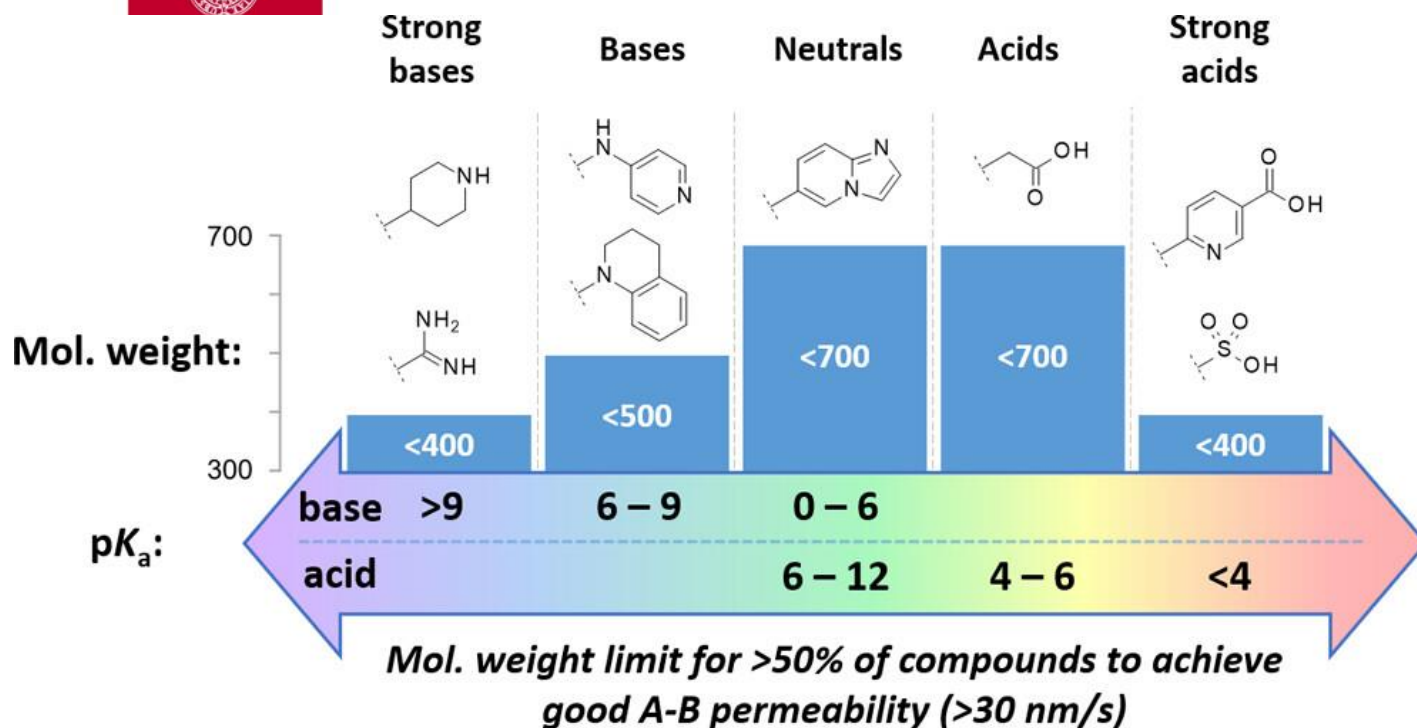
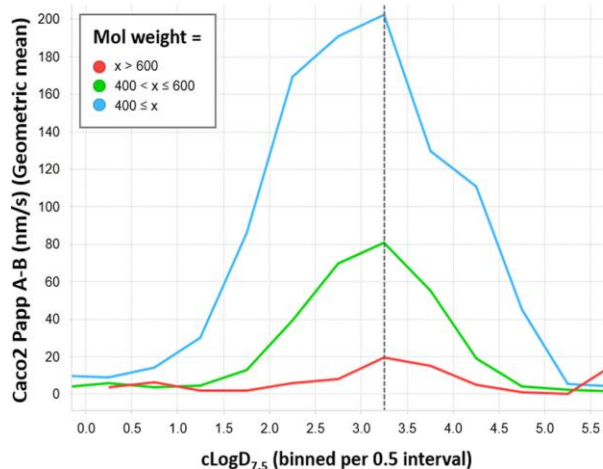


Figure 8. Molecular weight and pKa ranges at which >50% of compounds exhibit moderate to good permeability in the Caco2 Papp A-B assay (>30 nm/s). pKa values are stated for the most basic and the most acidic centers in a compound.

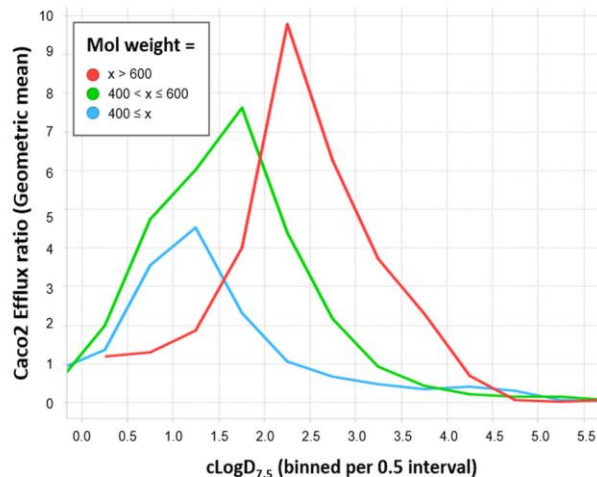
J. Med. Chem. 2023, 66, 4, 2347-2360

Trends in Molecular Properties, Bioavailability, and Permeability across the Bayer Compound Collection (O'Donovan et al.)

Caco2 Papp A-B (nm/s) vs cLogD_{7.5}



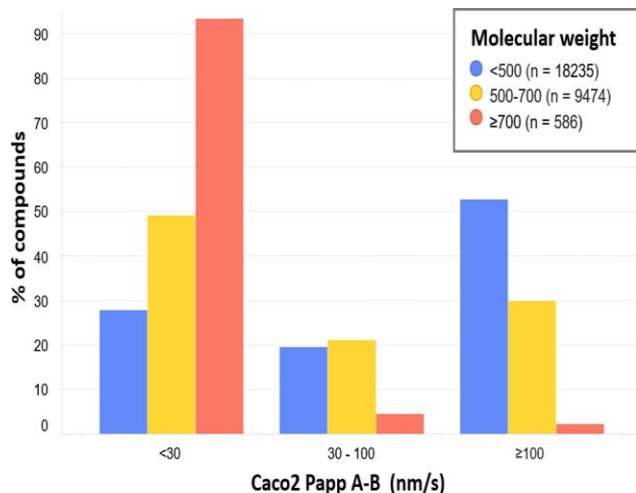
Caco2 Efflux ratio vs cLogD_{7.5}



(Left) Relationship between cLogD_{7.5} and geometric mean of Caco2 Papp A-B (nm/s), binned per 0.5 interval of cLogD_{7.5}.

Lines are colored by molecular weight range (blue = ≤400, green = 400–600, red = >600). Extreme values have been omitted as outliers

(Right) Relationship between cLogD_{7.5} and geometric mean of Caco2 efflux ratio, binned and colored as per left-hand figure



Bar chart showing the distribution of Caco2 apparent permeability A-B (nm/s) values for compounds with Ro5-like (<500), eRo5-like (500–700), and bRo5-like (≥700) molecular weights.

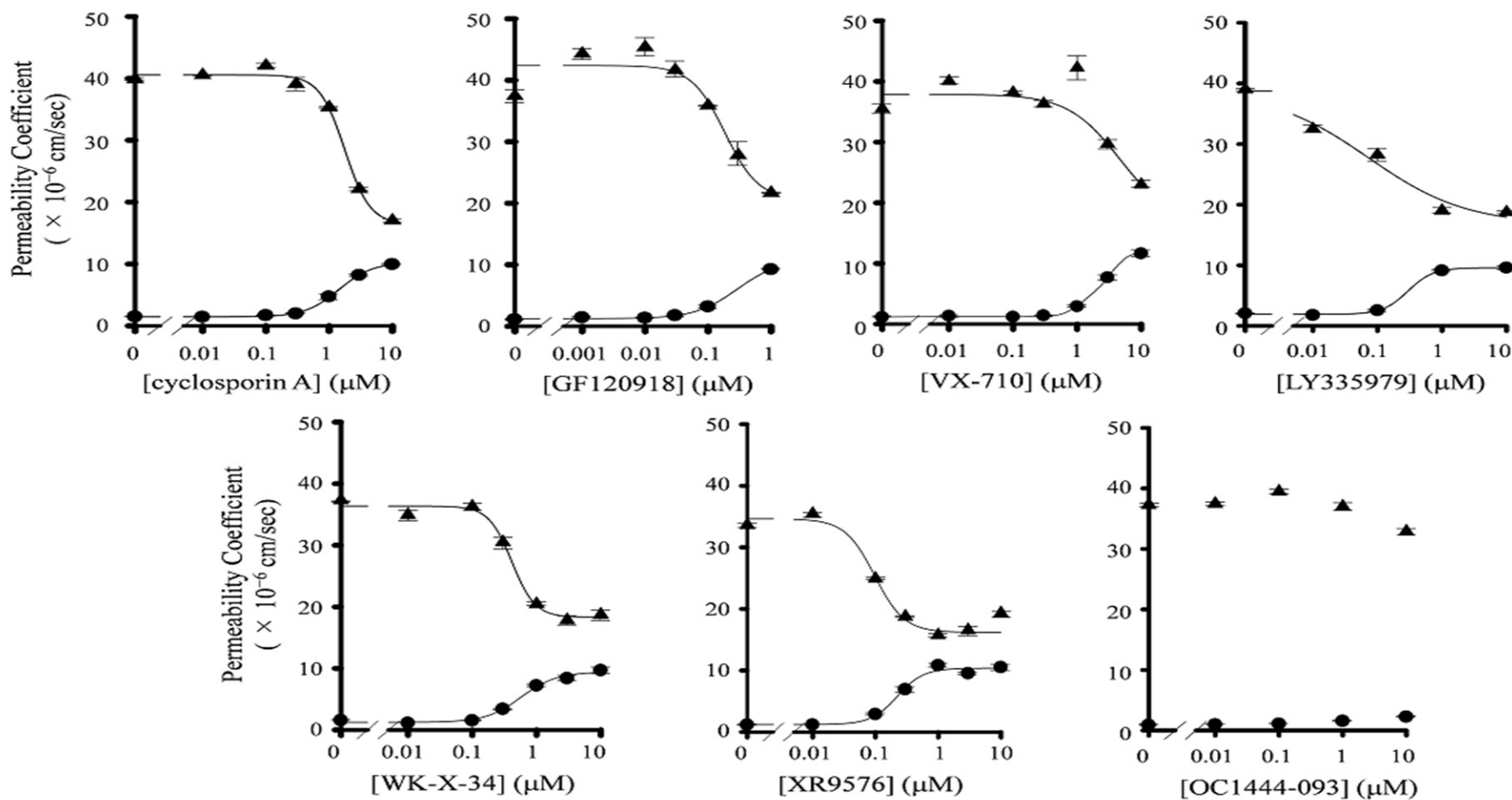
Interesting challenges for novel drug candidate beyond Lipinski rule of 5!

Recognized difficulties for *in vitro* permeability assessments for these larger and lipophilic drug candidates!



In vivo role of intestinal efflux

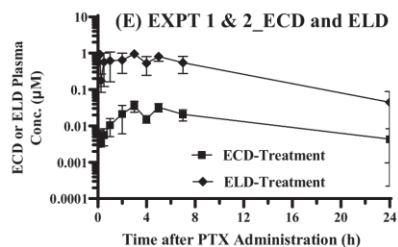
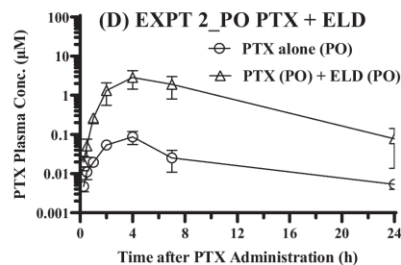
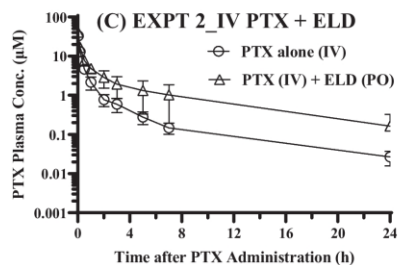
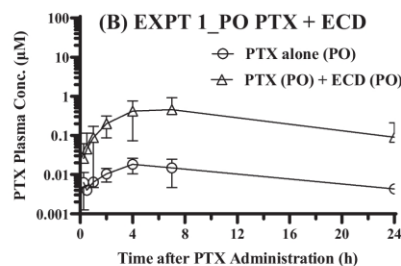
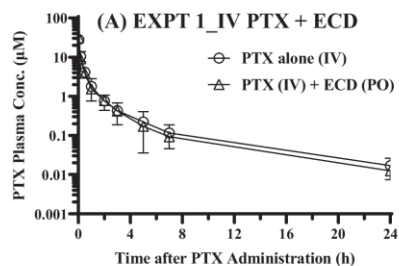
Inhibitory effect of P-gp inhibitors on P-gp-mediated efflux of paclitaxel in Caco-2 cells. The apical-to-basal (AP-to-BL) (●), and basal-to-apical (BL-to-AP) (▲).





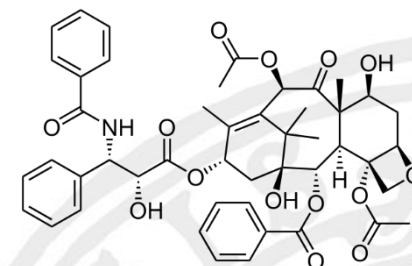
UPPSALA
UNIVERSITET

Evaluation of Encequidar (ECD) and Elacridar (ELD) as An Intestinal P-gp and BCRP Specific Inhibitors to Assess the Role of Intestinal P-gp and BCRP in Drug-Drug Interactions with paxlitaxel (PTX)



Chu J, Panfen E, Wang L, Marino A, Chen XQ, Fancher RM, Landage R, Patil O, Desai SD, Shah D, Xue Y, Sinz M, Shen H.

Pharm Res. 2023



Molar mass	853.91 g/mol
Log P	3.2-26
Hydrogen Acceptor Count	10
Hydrogen Donor Count	4
Physiological charge	0
Polar Surface Area	221.29 Å ²

Mean plasma concentration–time profile of PTX in rats after a single intravenous (IV; 5 mg/kg) or oral dose (PO; 20 mg/kg) of PTX alone (open circles) and following a single dose of PTX with oral ECD (A and B) or ELD (C and D) (open triangles)

In vitro models of intestinal epithelium: Toward bioengineered systems

Creff J et al Journal of Tissue Engineering
Volume 12: 1–16

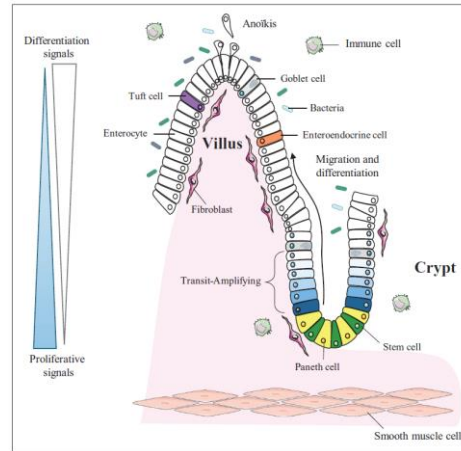


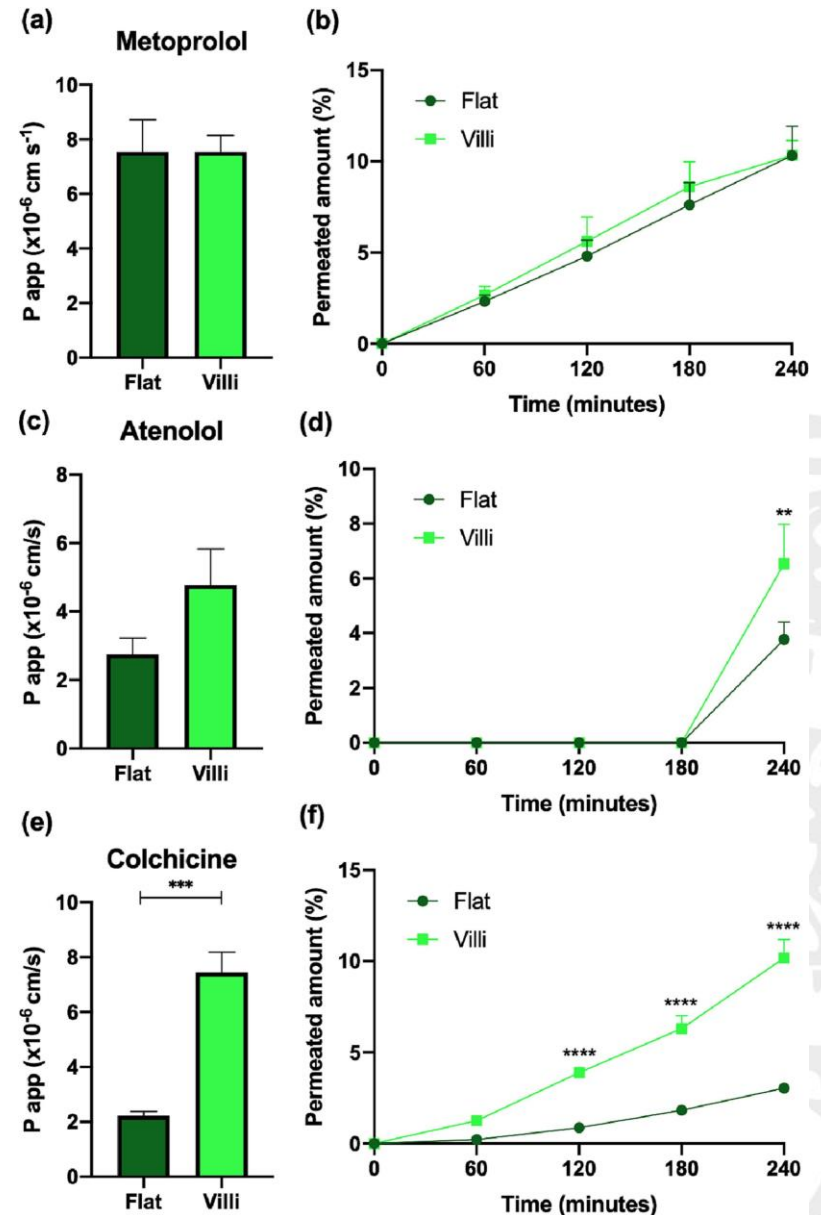
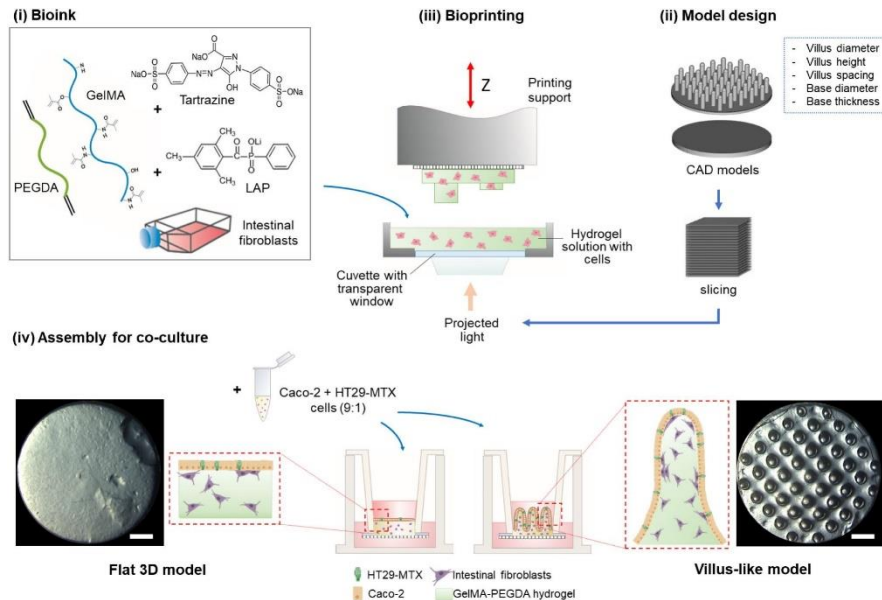
Table 1. Sources of cells to study intestinal physiology.

Cell source	Culture model	Advantages	Disadvantages	Applications
Adult stem cells Dissociated fresh crypt Dissociated organoids	Organoids 3D scaffolds Gut-on-chip 2D monolayer	Human or murine origin Heterogeneity	Adult stem cells Only epithelial cells	Genetic disease Drug screening Host/pathogen interaction Adult epithelial function Adult intestinal stem cell biology Tissue engineering
Pluripotent stem cells (iPS)	Organoids Gut-on-chip	Human origin Presence of mesenchyme Recapitulate the development	Immature features require maturation in vivo or <i>in vitro</i>	Genetic disease Drug screening Host/pathogen interaction Organ development Tissue interaction Tissue engineering
Cancer cell lines Caco-2 Caco-2/HT29 SW480	2D monolayer transwell 3D scaffolds Gut-on-chip	Human origin Easy and more affordable	Lack of heterogeneity Cancer origine	Cellular and molecular biology Absorption and toxicology assays Host/pathogen interaction Tissue engineering

Future in vitro intestinal permeability models?

The shape of our gut:
Dissecting its impact on drug
absorption in a 3D bioprinted
intestinal model

Macedo MH, et al . *Biomater Adv.* 2023
20;153:213564.



Conclusion

- Regional human intestinal P_{eff} identified as one important factor for future determinations.
- It seems as open system provides higher P_{eff} than double balloon approach – novel capsule systems (external controlled) and long GI-tube methodologies are developed and tested.
- *In vivo* colon P_{eff} of special urgency – but very difficult.
- *In vitro* intestinal P_{app} -values in the Ussing and 2D cell monolayer models need scaling and adjustment prior use in PBBM.
- The permeability model is important for the assessment of effect of excipients.
- Future intestinal organoids and 3D bioengineered intestinal models exhibit morphological and physiological features that resemble the native intestinal mucosa.
- New and interesting challenges ($MM > 700$ and $\log D > 5$) for novel drug candidate - beyond Lipinski's rule of 5! Require model development!
- It is expected there will be exciting and prosperous time for novel drug delivery systems
- Encequidar (ECD) and Elacridar (ELD) may be very useful as tool for assessment of intestinal efflux (P-gp and BCRP).
- The future role of molecular dynamic simulation and of artificial neural network models to predict the effective permeability of oral drugs before synthesis and even allow for optimization of relevant physicochemical properties of new molecules of interest.